Journal of Organometallic Chemistry, 449 (1993) 77–84

JOM 23369

Raman spectroscopic studies of gas phase Me_3In, Et_3In and $EtMe_2In$

Z.S. Huang, Chinho Park and T.J. Anderson

Department of Chemical Engineering, University of Florida, Gainesville, FL 32611 (USA)

(Received August 3, 1992)

Abstract

Gas phase Raman spectra were studied in detail for the first time for trimethylindium (Me_3In), triethylindium (Et_3In) and ethyl-dimethylindium ($EtMe_2In$). The analysis of these spectra indicates that all three compounds are monomeric in the gas phase. An accurate determination of the vibrational frequencies also was obtained for these compounds from the spectral analysis. While no indication of the presence of an impurity could be found in the Me_3In and Et_3In spectra, spectral features attributable to Me_3In were identified in the $EtMe_2In$ Raman spectrum, indicating that ligand rearrangement reaction occurs in the $EtMe_2In$ sample under our experimental conditions ($T > 55°C$). The implication of these results to the investigation of the pyrolysis mechanism of these compounds is discussed.

1. Introduction

There has been increasing interest in the application of optical diagnostic techniques to the study of organometallic vapor phase epitaxy (OMVPE) processes [1], particularly in the area of growth mechanism studies and real time *in situ* monitoring of the growth process. Such optical diagnostic techniques involve probing well-known spectral features characteristic of the species of interest. Therefore, it is important to define the spectroscopy of these species before such methods can be applied to OMVPE in a useful way.

Trimethylindium (Me_3In), triethylindium (Et_3In) and ethyl-dimethylindium ($EtMe_2In$) are the common indium source molecules used in OMVPE deposition of In containing semiconductors. Although their UV spectra have been studied in some detail [2], the vibrational spectra have not been thoroughly investigated. For Me_3In, the gas phase infrared spectrum and the liquid phase Raman spectrum have been investigated by Hall *et al.* [3]. More recently, Raman scattering and X-ray crystallographic results also were reported for solid Me_3In [4]. The molecular structure of this compound in the gas as well as in condensed phases is well understood. The gas phase Raman spectrum, however, has not been reported. That is, the vibrational frequencies which are only allowed in the Raman spectrum have not been previously measured for gaseous Me_3In.

The authors are unaware of studies in which the vibrational spectra of Et_3In were extensively investigated. Gas phase studies of Et_3In are particularly difficult to perform due to the low vapor pressure of this compound. This, in addition to the high reactivity of the compound, contributes to the lack of its spectroscopic characterization in the gas phase.

$EtMe_2In$ is a recently developed precursor for use in OMVPE processes and its physical and chemical properties have not been fully investigated. Although this source has shown promise for the growth of high quality epitaxial films, questions remain with regard to its purity and stability, particularly the tendency to undergo ligand exchange reactions. An early study by variable temperature ^1H NMR indicates that a ligand exchange reaction occurs for $EtMe_2In$ in solution [5]. On the other hand, conflicting mass spectrometric results were obtained by two different groups [6,7]. In view of these controversies, there are incentives for performing a Raman scattering investigation of this compound. Raman spectroscopy is a useful method for investigating the nascent constituents of a sample. It is advantageous in that the species are detected directly by identifying their characteristic spectral features without altering their chemical or physical state in the process.

Correspondence to: Dr. T.J. Anderson.

0022-328X/93/$6.00

In this study a detailed investigation of the Raman spectroscopy of Me_3In, Et_3In and $EtMe_2In$ was performed, yielding accurate values for the vibrational frequencies of these compounds. The possibility of using Raman spectroscopy to investigate the pyrolysis mechanism of these organometallic compounds is discussed. In addition, the stability of $EtMe_2In$ was investigated. Spectral features attributed to Me_3In were identified in the $EtMe_2In$ spectrum. These observations will be discussed in relation to the purity and liability of Et_2MeIn.

2. Experimental details

The present experimental apparatus has been successfully used previously for optical investigation of flow dynamics related to OMVPE processes [8]. A brief description of this system will be given here. A schematic diagram of the Raman spectrometer system is shown in Fig. 1. A Coherent Innova 90-5 Argon ion laser provided the excitation light for the Raman scattering. The laser line at 487.986 nm was used for the present experiment. The total laser power output was stabilized at 1 watt for each experiment. The slits of the double monochromator were opened to a width of 500 μm, corresponding to a resolution of approximately 5 cm^{-1}. Further reduction of the slit width did not yield better resolved fine structures in the recorded spectra. The absolute frequency was established using the N_2 vibrational Raman transition at 2331 cm^{-1} as the internal standard. Relative frequency calibration was obtained using factory-calibrated dispersion of the grating and stepping motor and was specified by the manufacturer to have an accuracy of ± 1 cm^{-1} over a scan of 5000 cm^{-1}. The polarization of the Raman scattering was not analyzed. Therefore, the accuracy of the frequency determination is approximately ± 1 cm^{-1}.

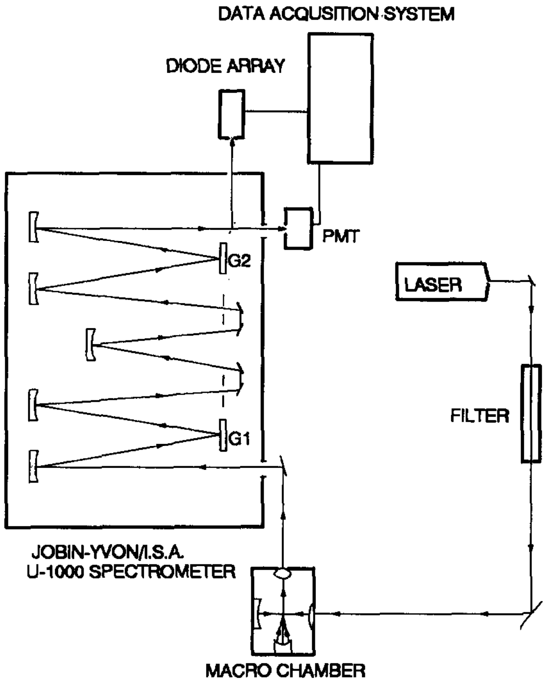

Fig. 1. Schematic drawing of the Raman spectrometer system. G1 and G2 are 1800 grooves/mm gratings blazed at 500 nm. An image-intensified photo-diode array (Princeton Instruments IRY-700) is also shown and was not used in the current experiment. A PMT (photomultiplier tube) operating in the photon counting mode was employed as the scattered light detector throughout this investigation. It is also noted that the excitation laser beam undergoes two passes through the probed volume and the scattered light is collected perpendicular to the excitation light direction. The OMVPE reactor, not shown, is located inside the sample chamber.

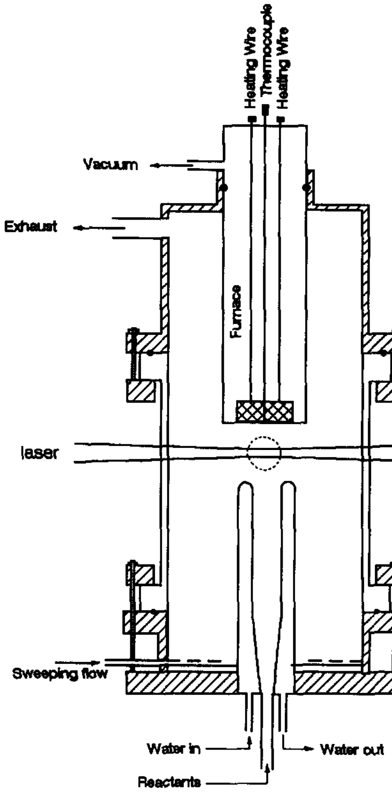

Fig. 2. Schematic diagram of the modified upflow OMVPE reactor. It is also noted that the excitation laser is focused in the center of reactant stream and the Raman scattering light is collected in a perpendicular direction.

A schematic of the custom upflow impinging jet OMVPE reactor that served as the optical gas cell in the present experiment is shown in Fig. 2. The reactor design provided two separate gas inlet streams of circular geometry; a center stream and a sweeping stream. The center flow contained the In source molecules that were delivered by saturating a carrier gas with the organometallic compounds. The sources were contained in commercial OMVPE bubblers and the gas flows were regulated with mass flow controllers. The sweeping stream contained the pure carrier gas and was used to avoid recirculation flows [9] as well as to reduce wall deposition of the organometallic compounds in the center flow.

The bubblers containing the organometallic sources were submerged in a constant temperature bath. The reactor incorporated a hot-water jacket surrounding the center inlet tube. The stainless steel tubing connecting the bubbler to the reactor was also maintained at an elevated temperature by using heating tapes. Typically, the inlet tube and transport line were maintained at a temperature 10 to 20°C higher than the bubbler temperature to prevent condensation during transport. The furnace also was maintained at 80°C. The excitation laser was adjusted to intercept the center flow stream 2 to 3 mm above the center inlet position to sample the vapor phase before significant recondensation occurred. The In precursors used in this study were of semiconductor grade and used without further purification. The Me_3In was purchased from Texas Alkyls, while Et_3In and $EtMe_2In$ were purchased from Alpha Products. The carrier gas used was N_2 or H_2 of ultra-high purity.

3. Results and discussion

3.1. TMIn

Among the three indium source compounds examined in this study, Me_3In has received the most attention spectroscopically. The infrared spectrum of gas phase Me_3In and the Raman spectrum of this species in the liquid phase has been studied in detail by Hall *et al.* [3], and a thorough vibrational analysis also was given. A brief discussion of their analysis is provided below to assist the discussion of the Me_3In spectral analysis as well as that of Et_3In and $EtMe_2In$ in the subsequent sessions.

Following the discussion of Hall *et al.* [3], the three methyl groups are considered as point masses owing to their unhindered internal rotation Hence, the vibrational spectra are characterized by an effective D_{3h} point group since the InC_3 skeleton is expected to be planar. The InC_3 skeleton vibrations consist of a symmetric stretch (a_1'), an anti-symmetric stretch (e'), an in-plane bending (e'), and an out-of-plane bending (a_2'') vibration. Among these, the a_1' vibration is only Raman active, the e' vibrations are both Raman and IR active, and the a_2'' vibration is only IR active. Therefore, it is expected to observe three InC_3 vibrations in the Me_3In Raman spectrum. An assessment of the line shapes for these transitions is obtained from the discussion of the rotational selection rules given by Herzberg [10]. A $\Delta K = 0$ type selection rule is expected for the a_1' vibration, giving rise to strong and sharp line-like features, while a $\Delta K = \pm 2$ selection rule is expected for the e' vibrations, yielding broad and band-like transitions.

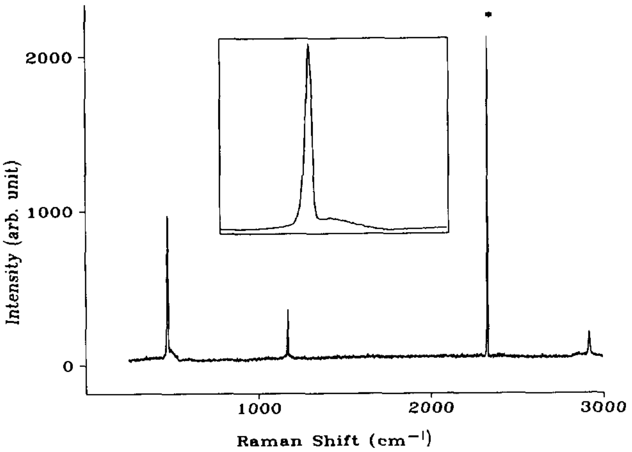

Fig. 3. Raman spectrum of gaseous Me_3In using N_2 as carrier gas. The transition marked with an asterisk is due to the 2331 cm^{-1} vibration of the carrier N_2 gas. This transition was also used as an absolute frequency calibration. The insert displays a slower scan of InC_3 stretch vibration, which shows more clearly the broad spectral feature due to the anti-symmetric In–C stretch.

In addition to a determination of the vibrational frequencies not observed in the previous gas phase IR study [3], part of the motivation for the present study lies in exploring the potential of using Raman spectroscopy to investigate the decomposition mechanisms of these organometallic compounds. The Raman spectrum of gaseous Me_3In is shown in Fig. 3. The spectrum was recorded with a time constant of one second per datum and the entire spectrum was scanned in less than one hour. The temperature of the Me_3In source was maintained at 45°C, corresponding to a Me_3In partial pressure of 11 Torr. It is evident from the spectrum that the signal to noise ratio is large for several of the observed transitions, suggesting the possibility of measuring thermal decomposition rates by Raman spectroscopy.

The observed spectrum can be understood on the basis of the vibrational analysis given above. Figure 3 shows that the In–C stretch vibrational transitions occurring near 500 cm^{-1} consist of two features. The sharp feature is assigned to the symmetric stretch (a_1'), while the broad shoulder is associated with the anti-symmetric stretch (e') vibration. The in-plane bending vibration (e') is observed at 113 cm^{-1} (shown in Fig. 4) which displays a broad band-like contour in agreement with the above analysis. Also included in Fig. 4 are the In–C stretch vibrations for relative intensity compari-

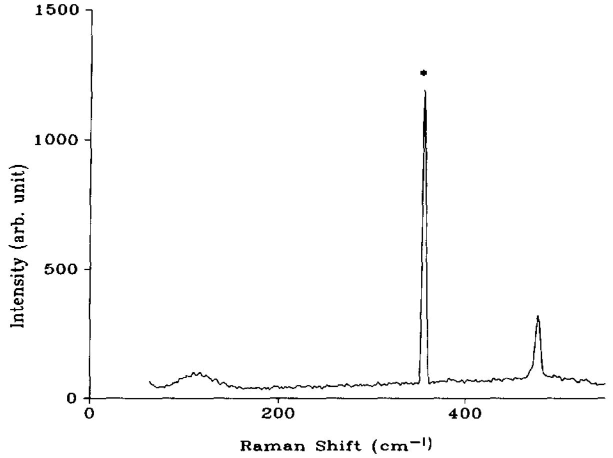

Fig. 4. Raman spectrum displaying in-plane bending vibration at 113 cm^{-1}. Spectrum was recorded using H_2 as the carrier gas and the transition marked with an asterisk is due to the H_2 rotational transition at 354.4 cm^{-1}.

son. Caution should be exercised in comparing the intensities since a slow reduction in the detection responsivity was observed during the scan due to a small amount of Me_3In condensation onto the optical windows. The features observed at 1173 cm^{-1} and 2925 cm^{-1} are associated with the symmetric bending and stretching vibrations of the methyl groups, respectively.

The vibrational frequencies obtained from the present study are summarized in Table 1, together with those of previous studies for comparison. The assignments are based on those given by Blake and Cradock [4]. It is noted that most transition frequencies determined in the present work were not observed in the previous IR work and hence the present study is complementary. The ν_{16} transition is broad and overlaps with the ν_3 transition in the Raman spectrum. Therefore, the value of 500 cm^{-1} determined in the IR study is believed to be more accurate. On the other hand, the value of 1173 cm^{-1} determined in this study should be more accurate for the ν_2 vibration.

TABLE 1. Comparison of Me_3In vibrational transition frequencies obtained from present work with those of previous investigations

Raman crystal [4]	Raman liquid [3]	Raman gas; this work	IR gas [3]	Assignments
86				
125	132vs, p	113s		$\nu_{17}e'$
155				
462vs	467vs	478vs		ν_3a_1'
480m				
488s	495s, dp	489s	500s	$\nu_{16}e'$
498s				
	635w, dp			$\nu_{20}e''$
			687ms	ν_9a_2''
	725w, dp		725s	$\nu_{15}e'$
1094m	1116m, br, dp			$\nu_{14}e'$
1123m				
1151s	1157s, p	1173vs	1155vw	ν_2a_1'
	2861w, sh		2860m	?
2915m	2910ms, p	2925vs		ν_1a_1'
			2920s	$\nu_s(CH_3)e'$
2975mw, br			3000s	$\nu_{as}(CH_3)a_2''$

3.2. Et_3In

The vibrational analysis of Et_3In is more complicated than that of Me_3In due to the complexity of the ethyl groups. Similar to the better characterized Group III triethyl compounds (*i.e.*, triethylborane [11] and triethylgallium [12]), the central In and the three attached carbon atoms are expected to lie on the same plane, while the locations of the three other carbon atoms and the fifteen hydrogen atoms are not certain due to hindered internal rotations. This complication makes it difficult to characterize the symmetry of this molecule. Although Jacques *et al.* [12] used a C_{3h} group to analyze the vibrational spectra of Et_3Ga, such an analysis cannot be considered unique. Because of the lack of sufficient spectral data (there is no previous report on the vibrational spectra of Et_3In in either the gas or condensed phases), a complete vibrational analysis was not attempted for Et_3In. Instead, the vibrations of a planar $In(C_2)_3$ skeleton are used to gain insight into the expected spectrum of this complicated molecule. In analogy to Me_3In, the ethyl groups are approximated as point masses and, consequently, the vibrational analysis is facilitated with an effective D_{3h} group. The result of such an analysis is identical to that given in the previous discussion of Me_3In.

The Raman spectrum of gas phase Et_3In is shown in Fig. 5. This spectrum was recorded with a bubbler temperature of 70°C corresponding to a vapor pressure of 5 Torr. The spectrum is strikingly similar to that of Me_3In and the simplicity of the spectrum is also indicative of the fact that Et_3In is monomeric in the gas phase. The transitions near 450 cm^{-1} are associated with the In–C stretch vibrations.

The sharp transition at 447 cm^{-1} is assigned to the In–C symmetric stretch, while the broad shoulder at 457 cm^{-1} (shown more clearly in the insert of Fig. 5) is assigned to the anti-symmetric In–C stretch. It is noted that the observed In–C stretch vibrational frequencies are only slightly smaller than those of Me_3In. This observation is unexpected since the ethyl group has a larger molecular weight. This apparent contradiction is attributed to a strong coupling between these vibrations and the ethyl group vibrations. Although it is not shown in Fig. 5, a broad transition was observed at 76 cm^{-1}, which is assigned to the in-plane bending vibration of the skeleton. It is noted that this frequency is

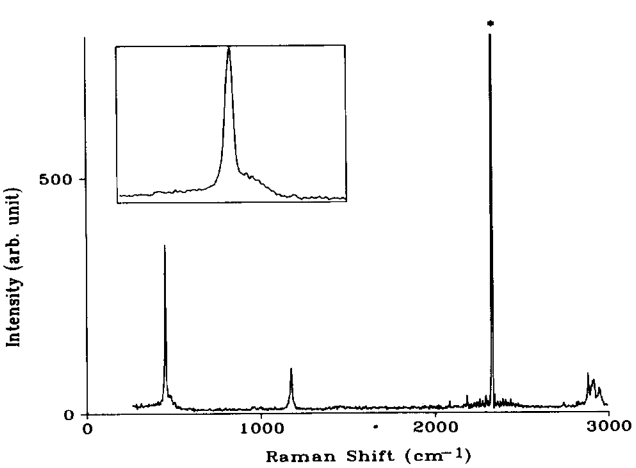

Fig. 5. Raman spectrum of gaseous Et_3In in N_2 carrier gas. The peak marked with an asterisk is due to the vibrational transition of the carrier. The small peaks seen close to this transition are due to rotational transitions associated with this vibrational band. Shown in the insert is a clearer view of the In–C stretch vibrational bands, displaying a sharp feature assigned to the symmetric In–C stretch and a broader band associated with the anti-symmetric In–C stretch.

considerably smaller than the corresponding one for Me_3In, consistent with the larger mass of the ethyl group.

Vibrations of the ethyl groups are complicated and a detailed vibrational analysis was not attempted. Instead, the approach taken by Lehmann *et al.* [11] in their analysis of triethylborane is used, in which only characteristic frequencies were assigned. The transition at 1174 cm^{-1} shown in Fig. 5 is associated with the C–H bending vibrations of the ethyl groups while the group of peaks near 2900 cm^{-1} are associated with the C–H stretching vibrations. A summary of the Et_3In transitions is given in Table 2.

3.3. $EtMe_2In$

There has been increasing interest in the development of $EtMe_2In$ as a substitute for the more commonly used precursors Me_3In and Et_3In in OMVPE. Since Me_3In is a solid at room temperature, the indium transport rate is subject to variation due to a slow recrystallization of the solid and subsequent reduction of the surface area. While Et_3In is a liquid source, it suffers from having a low vapor pressure and a tendency to participate in parasitic gas phase reactions. $EtMe_2In$, on the other hand, is a liquid at room temperature and has a reasonable vapor pressure (comparable to that of Me_3In). Indeed, $EtMe_2In$ has been used to grow a variety of semiconductor thin films with results comparable to those using Me_3In [6,13–15]. In addition, an investigation of the reproducibility of quantum well size over a period of six months indicates long-term stability of the $EtMe_2In$ source [15]. These results generally lead to the belief that $EtMe_2In$ is a viable and stable In-source for OMVPE processes.

TABLE 2. Raman transition frequencies of gaseous Et_3In and their vibration assignments

Raman shift (cm^{-1})	Assignments
76s	$In(C_2)_3$ in-plane deformation
447vs	$In(C_2)_3$ symmetric stretch
457s	$In(C_2)_3$ anti-symmetric stretch
1174s	CH_3, CH_2 symmetric deformation
2741w	CH_3, CH_2 stretch
2866w	CH_3, CH_2 stretch
2879s	CH_3, CH_2 stretch
2915s	CH_3, CH_2 stretch
2946s	CH_3, CH_2 stretch

The direct characterization of the $EtMe_2In$ physical and chemical properties, however, has been sparse in comparison and the results have been controversial. In particular, interest has focused on the tendency of $EtMe_2In$ to undergo a ligand exchange reaction to yield Me_3In as well as Et_3In or methyldiethylindium ($MeEt_2In$). In an early study of the purity of $EtMe_2In$, it was reported that neither Me_3In nor Et_3In could be detected by mass spectrometry [6]. In a later analysis by a variable temperature ^1H NMR, it was concluded that a rapid ligand exchange reaction occurs for $EtMe_2In$ in solution [5]. More recently, $EtMe_2In$ samples were investigated by Reents [7] using chemical ionization Fourier transform ion cyclotron resonance spectrometry. In this study, $EtMe_2In$ was found to contain 10% Me_3In and 18% $MeEt_2In$; the presence of Et_3In was not detected.

Having investigated the Raman spectroscopy of Me_3In and Et_3In, it is thought that characterization of $EtMe_2In$ by Raman spectroscopy would give an insight into the properties and purity of this compound. Raman spectroscopy can be used as direct and unambiguous means of identifying impurity species; the spectral features of Me_3In and Et_3In having been established in the preceding work.

The $EtMe_2In$ Raman spectrum is shown in Fig. 6, recorded at a bubbler temperature of 55°C. A first inspection of this spectrum suggests similarities with the spectra of Me_3In and Et_3In. The spectral feature near 470 cm^{-1} is characteristic of In–C stretch, while the transition at 1174 cm^{-1} and the cluster of transitions near 2900 cm^{-1} are characteristic of C–H bending and stretching vibrations of the alkyl groups, respectively. Before a more detailed examination of these spectral features is presented, however, it is instructive to perform a group theoretical vibrational analysis similar to that given in the preceding discussion of Me_3In and Et_3In.

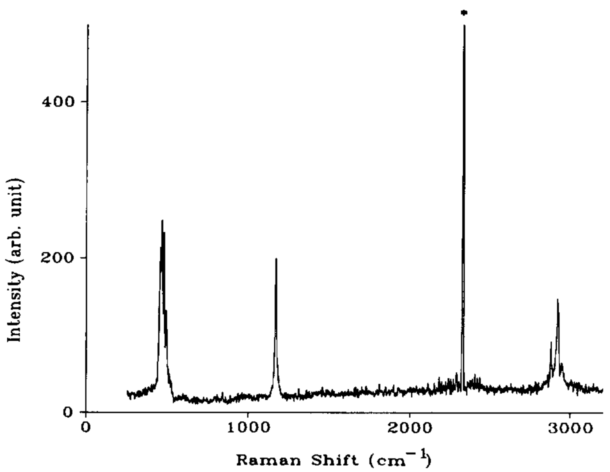

Fig. 6. Raman spectrum of gas phase $EtMe_2In$ in N_2 carrier gas. The peak marked with an asterisk is due to the N_2 carrier transition. It is seen that the main features of this spectrum are similar to those of Me_3In and Et_3In, though clear differences are evident.

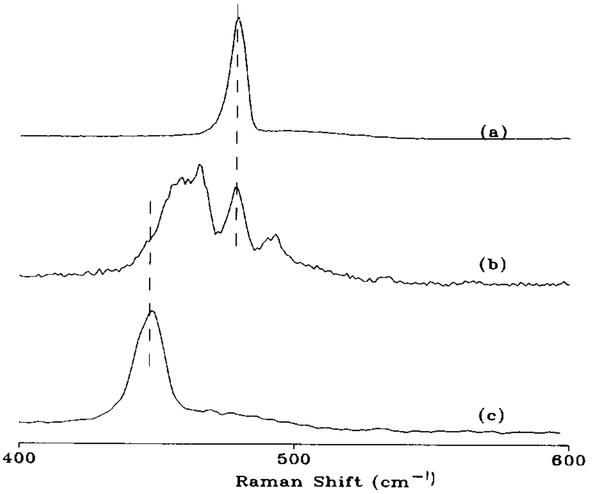

Fig. 7. A comparison of the spectral features of Me_3In (a), $EtMe_2In$ (b), and Et_3In (c) in the frequency region of In-C stretch vibrations. It is clear that the $EtMe_2In$ spectral features consist of more than three transitions. While the Me_3In transition closely matches one of these features, no match can be found for the Et_3In transition in $EtMe_2In$ spectrum.

In analogy to the analysis of Me_3In and Et_3In, the alkyl groups are approximated as point masses. In this case, however, a C_{2v} point group is used due to the presence of the ethyl group. With this group, the In–C stretch vibrations consist of three nondegenerate modes ($2a_1 + b_1$), in contrast to that for Me_3In and Et_3In. The in-plane bending vibrations also consist of two nondegenerate modes ($a_1 + b_1$) while the out-of-plane bending vibration is classified as of the b_2 symmetry. It also is noted that each of these vibrations is expected to be both IR and Raman active. Following the discussion given by Herzberg [10], the $\Delta K = 0$ rotational selection rule is expected for the a_1 vibrations, giving rise to sharp line-like features, while the $\Delta K = \pm 1$ selection rule is expected for the b_1 and b_2 vibrations, yielding broad vibrational bands.

Based on the above analysis, the finer details of the $EtMe_2In$ Raman spectrum are next examined, particularly those spectral features pertaining to the $InC(C_2)_3$ skeleton vibrations. Figure 7(b) displays an expanded view of the transitions associated with the stretching vibrations. It is seen that they give rise to four peaks. On the low frequency side there are two partially resolved sharp transitions at 456 and 465 cm^{-1}, respectively. The other two transitions consist of one sharp peak at 478 and a broader peak at 492 cm^{-1}. As pointed out in the preceding analysis, only three vibrational transitions are expected for $EtMe_2In$ in this frequency region. The presence of the additional peak is therefore indicative of the existence of an impurity.

To identify the nature of this impurity, these transitions are compared with the spectral features associated with Me_3In, Fig. 7(a) and Et_3In, Fig. 7(c) in this frequency region. It is noted that the Me_3In spectral feature closely matches the peak at 478 cm^{-1} in the $EtMe_2In$ sample, suggesting Me_3In is the impurity. To provide further supporting evidence for the presence of Me_3In, the other Me_3In spectral features are identified in $EtMe_2In$ spectrum, particularly the in-plane bending vibrations, that, as pointed out in the Et_3In discussion, are expected to be separated in frequency from the $EtMe_2In$ features. Such a comparison is shown in Fig. 8. It is clear from this figure that the Me_3In transition, shown in panel (a), exactly matches the peak at 113 cm^{-1} of the $EtMe_2In$ spectrum. Furthermore, a comparison between the frequency values

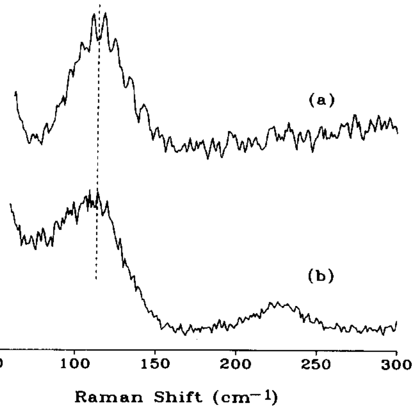

Fig. 8. A comparison of spectral features of the Me_3In sample (a) and the $EtMe_2In$ sample (b) in the region of InC_3 skeleton bending vibrations. It is seen that the Me_3In transition matches the peak at 113 cm^{-1} of the $EtMe_2In$ sample. The transition at 227 cm^{-1} in the $EtMe_2In$ spectrum is tentatively assigned to the out-of-plane bending vibration of the skeleton.

TABLE 3. Raman transition frequencies of gaseous $EtMe_2In$ sample and their vibration assignments. Note that some of the transitions were attributed to Me_3In

Raman (cm^{-1})	Assignments
113s	Me_3In
227m	out-of-plane deformation
456s	skeleton symmetric stretch
465s	skeleton symmetric stretch
478s	Me_3In
492s	skeleton anti-symmetric stretch
1174s	CH_3, CH_2 deformation
2883m	CH_3, CH_2 stretch
2923s	CH_3, CH_2 stretch
2946m	CH_3, CH_2 stretch

listed in Table 1 and the values listed in Table 3 (summarizing the frequencies of all transitions in the $EtMe_2In$ sample) indicates that exact matching is found for the methyl group vibrations of Me_3In. In this case, however, the two Me_3In transitions overlap those associated with $EtMe_2In$. Although the transition associated with the In–C anti-symmetric stretch of Me_3In is not prominent in the $EtMe_2In$ spectrum, its presence is evidenced by the fact that the high-frequency wing of the transitions in Fig. 7(b) extends towards higher frequency, consistent with that of Me_3In.

Having established the presence of Me_3In, progress can be made towards the assignment of the transitions pertaining to $EtMe_2In$. The two partially resolved sharp peaks at 456 and 465 cm^{-1} are assigned to the two In–C stretching vibrations of a_1 symmetry, while the broader peak at 492 cm^{-1} is associated with the In–C stretch vibration of b_1 symmetry. The broad peak at 227 cm^{-1} is tentatively associated with the out-of-plane bending vibration. The transitions near 1174 cm^{-1} and 2900 cm^{-1} are associated with bending and stretching vibrations of the alkyl groups. These results are summarized in Table 3.

It is interesting that the results of the present study are in good agreement with those of the previous study by Reents [7], who also detected a significant amount of Me_3In in the $EtMe_2In$ sample. It is noted that the presence of Et_3In is not significant in an $EtMe_2In$ sample, as is indicated by the lack of Et_3In spectral features (see Fig. 7, for example) in the $EtMe_2In$ spectrum. This also is in agreement with the analysis by Reents. Nevertheless, the presence of $MeEt_2In$ reported by Reents cannot be identified in the present study. The inability to detect this species is attributed to its relatively low vapor pressure since the gas phase is dominated by the more volatile species Me_3In and $EtMe_2In$.

Before closing the discussion on the results of probing $EtMe_2In$, it should be emphasized that this same $EtMe_2In$ sample was used to successfully grow InGaP thin films with device quality results [13]. Care should be taken in interpreting the results of the present study since the experiment was carried out at an elevated temperature (55°C bubbler temperature and approximately 80°C gas line temperature). Although it seems clear that ligand exchange reaction products can be detected at such conditions, it is not apparent from the present study whether the ligand exchange reaction occurs in the gas phase or in the liquid phase. Neither can the present study discern whether such reaction(s) occurs at milder conditions (*e.g.*, below room temperature). It also is possible that this sample was not pure in its original form, as suggested by Reents [7]. Further investigation is underway to answer these questions as well as to examine the influence of this reaction on In incorporation mechanisms during OMVPE.

4. Conclusions

A detailed study of the gas phase Raman spectra has been carried out for the first time for Me_3In, Et_3In and $EtMe_2In$. The results indicate that all three compounds are monomeric in the gas phase. While both the Me_3In and Et_3In samples are pure and stable, the $EtMe_2In$ sample was observed to contain a significant amount of Me_3In. This suggests that either the $EtMe_2In$ compound becomes unstable and undergoes a ligand exchange reaction(s) under our experimental conditions (55°C for the liquid phase and 80°C for the gas phase), or this compound was not pure in its original form. The results of the present investigation, together with those of the previous studies, seems to raise questions concerning the stability and purity of the $EtMe_2In$ source even under milder conditions. It is also conceivable that the ligand exchange reaction of $EtMe_2In$ could play a positive role in facilitating indium incorporation of OMVPE thin film growth, since the growth studies suggest this source is a promising precursor for epitaxial deposition of compound semiconductors.

Acknowledgments

The authors are indebted to Dr. Balu Pathangey for many enlightening discussions. Mr. Peter Axson is also thanked for his diligent technical assistance.

References

1 W. Richter, P. Kurpas, R. Lückerath, M. Motzkus and W. Waschbüsch, *J. Crystal Growth, 107* (1991) 13.
2 H. Okabe, M. K. Emadi-Babaki and V. R. Mcrary, *J. Appl. Phys., 69* (1991) 1730.

3 J. A. Hall, L. A. Woodward and E. A. V. Ebsworth, *Spectrochim. Acta*, 56 (1964) 1249.

4 A. J. Blake and S. Cradock, *J. Chem. Soc., Dalton Trans.*, (1990) 2393.

5 D. C. Bradley, H. Chudzynska and D. M. Frigo, *Chemtronics, 3* (1988) 159.

6 K. L. Fry, C. P. Kuo, C. A. Larsen, R. M. Cohen, G. B. Stringfellow and A. Melas, *J. Electron. Mater., 15* (1986) 91.

7 W. D. Reents, Jr., *Anal. Chim. Acta, 237* (1990) 83.

8 C. H. Park, A. Zhao, Z. S. Huang and T. J. Anderson, to be published.

9 G. Wahl, *Thin Solid Films, 40* (1977) 13.

10 G. Herzberg, *Infrared and Raman Spectra of Polyatomic Molecules*, D. Van Nostrand Company, Inc., New York, 1945.

11 W. J. Lehmann, C. O. Wilson, Jr. and I. Shapiro, *J. Chem. Phys.*, *28* (1958) 781; 31 (1959) 1071.

12 M. J. Chouteau, G. Davidovics, F. D'Amato and L. Savidan, *Compt. Rend., 260* (1965) 2759.

13 K. C. Chou, H. D. Lee, B. Pathangey, T. J. Anderson and A. Melas, to be published.

14 J. Knauf, D. Schmitz, G. Strauch, H. Jürgensen, M. Heyen and A. Melas, *J. Crystal Growth, 43* (1988) 34.

15 P. K. York, K. J. Beernink, J. Kim, J. J. Coleman, G. E. Fernandez and C. M. Wayman, *Appl. Phys. Lett., 55* (1989) 11.